Biochemical and Biophysical Research Communications 504 (2018) 40–45

Contents lists available at ScienceDirect

Biochemical and Biophysical Research Communications

journal homepage: www.elsevier.com/locate/ybbrc

Structural and biochemical studies on the role of active site Thr166 and Asp236 in the catalytic function of D-Serine deaminase from *Salmonella typhimurium*

Geeta Deka [a], Sakshibeedu R. Bharath [a], Handanhal Subbarao Savithri [b], Mathur Ramabhadrashastry Narasimha Murthy [a, *]

[a] Molecular Biophysics Unit, Indian Institute of Science, Bangalore, 560012, India
[b] Biochemistry Department, Indian Institute of Science, Bangalore, 560012, India

ARTICLE INFO

Article history:
Received 7 August 2018
Accepted 17 August 2018
Available online 30 August 2018

Keywords:
Salmonella typhimurium
PLP binding
X-ray crystal structure
D-ser
Active site

ABSTRACT

D-Serine deaminase (DSD) degrades D-Ser to pyruvate and ammonia. Uropathogenic bacteria survive in the toxic D-Ser containing mammalian urine because of DSD activity. The crystal structure of the apo form of *Salmonella typhimurium* DSD (*St*DSD) has been reported earlier. In the present work, we have investigated the role of two active site residues, Thr166 and Asp236 by site directed mutagenesis (T166A and D236L). The enzyme activity is lost upon mutation of these residues. The 2.7 Å resolution crystal structure of T166A DSD with bound PLP reported here represents the first structure of the holo form of *St*DSD. PLP binding induces small changes in the relative dispositions of the minor and major domains of the protein and this inter-domain movement becomes substantial upon interaction with the substrate. The conformational changes bring Thr166 to a position at the active site favorable for the degradation of D-Ser. Examination of the different forms of the enzyme and comparison with structures of homologous enzymes suggests that Thr166 is the most probable base abstracting proton from the Cα atom of the substrate and Asp236 is crucial for binding of the cofactor.

1. Introduction

D-amino acids such as D-Ala and D-Glu are components of bacterial cell walls [1]. Although D-Ser is toxic, most bacteria survive and propagate in D-Ser containing media by degrading D-Ser to pyruvate and ammonia (Scheme 1), a reaction catalyzed by D-Serine deaminase (DSD, encoded by dsdA gene). Uropathogenic bacteria such as *S. saprophyticus* and *E. coli* (UPEC) survive in D-Ser containing urine due to the action of DSD [2] [3]. D-Ser also plays an important role in regulating the N-methyl-D-aspartate (NMDA) subtype of glutamate receptor [4].

DSD (EC 4.3.1.18) belongs to fold type II or tryptophan synthase β (TRPSβ) family of pyridoxal 5′ phosphate dependent (PLP) enzymes. PLP is a versatile cofactor for a wide variety of enzymes that carry out elimination, replacement, transamination, decarboxylation and racemization reactions with amino acid substrates [5]. DSD has been biochemically characterized from *E. coli* [6,7], *Klebsiella* [8], *S. cerevisiae* [9] and chicken [10]. Crystal structures of DSD from *E. coli* (PDB code: 3SS7 [11]), *P. xenovorans* (PDB code: 3GWQ, Joint Center for Structural Genomics) and *S. typhimurium* (PDB code: 3R0Z [12]) have been determined. The *E. coli* DSD (*Ec*DSD) and *S. typhimurium* DSD (*St*DSD) are monomeric proteins unlike most of the fold type II PLP dependent enzymes such as 2, 3-Diaminopropionate ammonia lyase (DAPAL [13]), O-acetylserine sulfhydrylase (OASS [14]), which are dimers. Crystals of wild type *St*DSD (Wt-*St*DSD, PDB code: 3R0Z) and SeMet incorporated DSD co-crystallized in presence of isoserine (SeMet-*St*DSD, PDB code: 3R0X) belong to the space groups C2 and $P2_12_12$, respectively [12]. The structures of both these crystal forms represent the apo form of the enzyme. These structures suggested that the enzyme undergoes a large conformational change from an open to a closed conformation upon interaction with isoserine [12]. Based on these structures, it was suggested that Thr166 might be responsible for abstraction of proton from Cα atom of D-Ser in the catalytic reaction. It was also proposed that Asp236 might play a role in external aldimine formation [12]. However, because of lack of crystal structure of *St*DSD bound to the cofactor PLP, these proposals could

* Corresponding author.
E-mail address: mrn@iisc.ac.in (M.R.N. Murthy).

https://doi.org/10.1016/j.bbrc.2018.08.116
0006-291X/

Scheme 1. The degradation of D-Ser to pyruvate and ammonia by D-Serine deaminase, a PLP dependent enzyme.

not be validated further.

In this manuscript, we present the X-ray crystal structure of an active site mutant (T166A) of *St*DSD; representing the first PLP-bound (holo) form of the enzyme. We have carried out biochemical studies on the T166A and D236L mutants of DSD to understand the role of Thr166 and Asp236 in the function of DSD. The structural features that are important for catalysis are discussed in the light of these structural and biochemical investigations.

2. Materials and methods

2.1. Cloning, over-expression and purification of active site mutants

The gene for *St*DSD cloned in pET21b vector was used as the template for the generation of single site mutants [12]. Two active site residues Thr166 and Asp236 were targeted for mutagenesis (shown in red italics) using single primer extension method [15]. The primers were designed so as to contain a restriction site (shown in green italics) by choosing appropriate degenerate codons. The mutants were further confirmed by sequencing.

D236L: ctgtttctttatcgac*ctc**gag*aactctcgcacgc

T166A: gccgtcggttca*gcc**ggc*aatctgg

The two active site mutants of *St*DSD were over-expressed and purified using the protocol found suitable for the wild type enzyme [12]. The purified proteins corresponded to a size of 49 kDa when examined on a 12% SDS-PAGE.

2.2. Crystallization of StDSD

The purified proteins were incubated with 0.1% of n-octyl-β-glucopyranoside prior to setting up crystallization. Initial trials of crystallization were carried out at 298 K using the hanging drop method under the conditions found suitable for the wild type enzyme [12]. Crystals of mutant proteins (T166A and D236L) could not be obtained under this condition or with small variations of the condition. Therefore, screening for suitable conditions was carried out using a number of commercially available screens including Hampton Crystal screens 1 and 2, Index screens 1 and 2, Jena Basic screens 1–4 and Jena classic screens 1–10. No hits were obtained for D236L. However, crystals of T166A were obtained from 20% w/v polyethylene glycol 4,000, 100 mM MES pH 6.5, 600 mM sodium chloride (JBscreen classic 3/C2). These crystals were fragile and difficult to mount. The diffraction data obtained from the best crystal was used for structural studies.

2.3. X-ray diffraction data collection

A single crystal of *St*DSD-T166A was mounted on a cryo-loop and frozen in liquid nitrogen. X-ray diffraction data extending to 2.7 Å were recorded using a CCD image plate detector while maintaining a temperature of 100 K at the BM14 beamline at ESRF, Grenoble. The data were processed using the program iMOSFLM and scaled using SCALA of the CCP4 suite [16]. The crystal belonged to the space group C2 with unit cell parameters of a = 108.31 Å, b = 46.14 Å, c = 99.28 Å and β = 100.8°. Although the space group is the same, the unit cell parameters for the T166A mutant were different from those of the wild type enzyme (PDB code: 3R0Z) for which a = 100.02 Å, b = 46.79 Å, c = 100.04 Å and β = 93.75°.

2.4. Structure determination and refinement

The structure of *St*DSD-T166A mutant was determined by molecular replacement using Wt-*St*DSD (PDB code: 3R0Z) as the phasing model. All hetero atoms and water molecules of the phasing model were removed to avoid model bias. The solution obtained by PHASER [17] was first subjected to rigid body refinement and then subjected to positional refinement using Refmac5 of CCP4 suite [18]. Each cycle of refinement was followed by manual model building using COOT [19].

2.5. Spectral studies and activity assays

Spectral studies were carried out to monitor the formation of internal aldimine as well as the product pyruvate using a Jasco UV–Visible V-630 spectrophotometer. 1 mg/ml of protein in 50 mM HEPES pH 7.5, 100 mM NaCl buffer were used for the study. The reactions were initiated by addition of 1 mM of D-Ser and spectra were recorded in the range of 300–550 nm as a function of time.

The specific activities of the Wt-*St*DSD as well as the two active site mutants (T166A and D236L) were estimated using 2,4-dinitrophenyl hydrazine (DNPH) method by measuring the α-keto acid released during the reaction as described previously [12]. The reaction mixture was composed of 50 mM potassium phosphate buffer (pH 7.5), 50 μM PLP, 100 μM of the substrate D-Ser and 50 ng of enzyme.

3. Results

3.1. X-ray crystal structure determination of StDSD-T166A

All the diffraction datasets collected for T166A-DSD mutant crystals contained spots from polycrystalline contaminations making meaningful data processing very difficult. Only a single data set collected on a crystal of T166A which contained multiple ice rings that could be processed (Supplementary Fig. S1) by excluding the contaminating rings [20]. Because of the ice rings, the quality of the processed data was low. This is reflected in the data statistics (Table 1).

The structure of *St*DSD-T166A was determined by molecular replacement using the wild type structure as the phasing model from which all non-protein atoms were removed. The solution obtained was refined to a final R_{work} and R_{free} of 28.91% and 34.85%, respectively, using REFMAC5 of CCP4 suite [18]. The refinement statistics is listed in Table 2.

3.2. Quality of the model

Despite the limited resolution (2.7 Å) and data quality, a model (residues 2–439) of the mutant protein *St*DSD-T166A could be built into the final electron density map with 99.4% of the residues in the allowed regions of the Ramachandran map and only two residues (0.60%) in the disallowed region. Continuous electron density could be traced for most of the main chain as well as the side chain atoms with the exception of a few residues (69–73, 212–227 and the C-terminal hexa-histidine tag) where electron densities were either missing or fragmented. These residues have not been included in the final model.

Table 1
Crystal data collection statistics for *St*DSD-T166A mutant.

PDB ID	6AA9
Wavelength (Å)	0.95372
Space group)	C2
Unit cell parameters)	a = 108.31, b = 46.14, c = 99.28; β = 100.8°
Resolution range (Å))	53.20–2.70 (2.83–2.70)
No. of observed reflections)	49,193 (6733)
No. of unique reflections)	13,514 (1791)
Multiplicity)	3.6 (3.8)
R_{merge} (%)[a])	16.7 (22.1)
Completion (%))	99.9 (100.0)
<I>/<σI>)	6.1 (4.6)
Mathews coefficient (Å^3 Da^{-1}))	2.43
Solvent content (%))	49.38%
Content of the asymmetric unit)	Monomer

Values in parentheses correspond to the highest resolution bin.
[a] $R_{merge} = \sum_{hkl}\sum_i |I_i(hkl) - \langle I(hkl)\rangle| / \sum_{hkl}\sum_i I_i(hkl)$. where $I_i(hkl)$ is the intensity of the i^{th} observation of reflection *hkl and* $\langle I(hkl)\rangle$ is the weighted average intensity.

Table 2
Refinement statistics for *St*DSD-T166A mutant.

R_{work} (%)[b]	28.91
R_{free} (%)[c]	34.85
No of atoms	
Protein	3104
Water	158
Ligands	6
Average B-factor (Å^2)	
Protein	19.08
Water	19.70
Ligands	32.39
RMSD from ideal values	
Bond length (Å)	0.005
Bond angle (°)	0.912
Ramachandran plots (%)	
Most favoured	92.3
Additionally allowed	7.1
Generously allowed	0.0
Disallowed	0.6

[b] R_{work} (%) = $(\sum_{hkl}|F_o - F_c|)/\sum_{hkl}F_o$, F_o and F_c are observed and calculated structure factor amplitudes.
[c] R_{free} (%) is defined in the same way as R_{work} and refers to randomly selected 5% of the reflections not used for refinement.

3.3. Interactions of the cofactor (PLP) with the active site residues

The *St*DSD-T166A mutant was crystallized in its monomeric form with one molecule in the crystal asymmetric unit. The overall topology of the mutant, as expected, agrees closely with the wild type as well as the SeMet-*St*DSD structures (RMSD ~1 Å). The monomeric *St*DSD-T166A has a large (residues 1–42, 76–108 and 239–440) and a small domain (residues 43–75 and 109–238) like the wild type enzyme. Significant electron density for a bound PLP could be located at the active site. The PLP is bound at the beginning of the helix H7 (Ile115-135Ala) at the interface of the two domains via a Schiff base linkage with the ε-amino group of Lys116. The pyridine ring of PLP is held in a hydrophobic cavity between Ile115 and Leu338. The hydroxyl group at C_3 of PLP is hydrogen bonded (3.22 Å) to Asn168 and the N_1 of the pyridine ring of PLP is hydrogen bonded (2.90 Å) to Thr422. The 5′ phosphate group of PLP is stabilized by a Gly-rich loop or PLP binding loop as observed in all other PLP dependent enzymes [21]. The PLP is anchored by hydrogen bonding interactions between the main chain nitrogen atoms of Gly277, Val278, Gly279, Gly280, Gly281 and the 5′ oxygen atoms of the phosphate group of PLP. The interactions that stabilize the PLP cofactor at the active site are shown in Fig. 1.

Structural superposition of the active sites of Wt-*St*DSD, SeMet-*St*DSD and *St*DSD-T166A (Fig. 2) reveals that the orientations of most of the active site residues that interact with the cofactor PLP are preserved. In both the apo forms of DSD, a sulfate molecule was observed at a place corresponding to the 5′ phosphate of PLP. A movement of ~4.2 Å is observed in the Nε atom of Lys116 between the Wt-*St*DSD and the SeMet-*St*DSD obtained in the presence of isoserine. The active site is much less accessible to the solvent in the closed form represented by SeMet-*St*DSD due to the well structured segment 234–239 that partially blocks the active site. In the apo form represented by Wt-*St*DSD, this segment is disordered and the active site becomes much more accessible to PLP and the substrate. Thus the substrate may enter the active site in the open conformation while catalysis may take place in the closed conformation.

A metal ion (Na^+) bound close the active site was observed in SeMet-*St*DSD [12]. In *St*DSD-T166A crystal structure also electron density at a corresponding position was observed. Based on geometry and interactions with nearby residues, the density has been attributed to a Na^+ ion. The metal ion is probably acquired from the purification buffer. It is coordinated with a number of residues

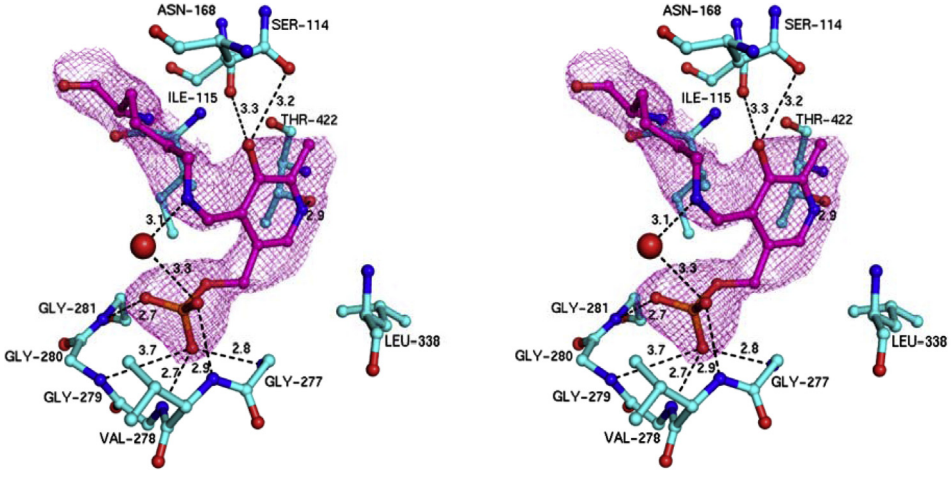

Fig. 1. Stereodiagram showing interactions of the cofactor PLP (pink ball and stick) with the active site residues (cyan ball and stick) in *St*DSD-T166A. Inter atomic distances in Å are shown on black dashed lines connecting the atoms. The electron density for PLP (*2mFo-DFc* contoured at 1.0 σ) is shown as a pink mesh. (For interpretation of the references to colour in this figure legend, the reader is referred to the Web version of this article.)

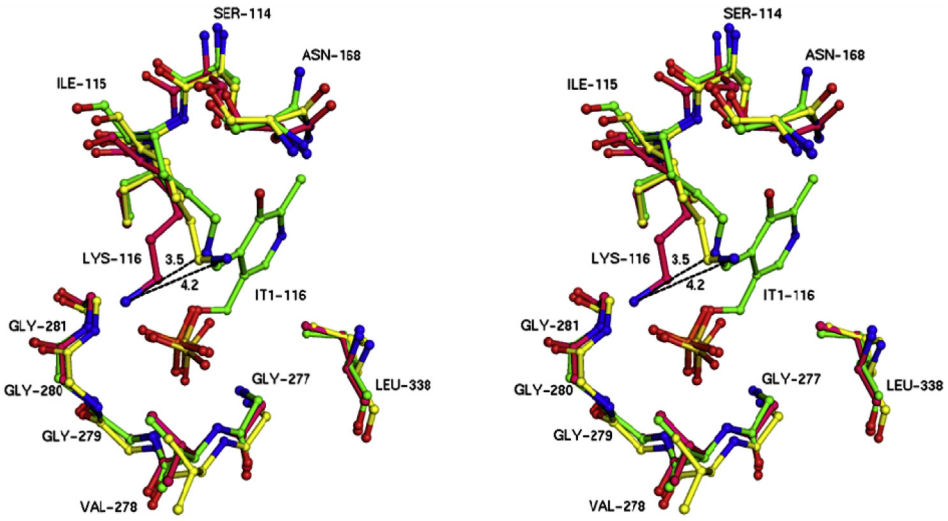

Fig. 2. Stereodiagram showing structural superposition of the active sites of apo- *St*DSD (3R0Z, yellow ball and stick), SeMet-*St*DSD after interaction with isoserine (3R0X, pink ball and stick) and holo-*St*DSD-T166A (green ball and stick). The change in the position and conformation of Lys116 between the open (apo- *St*DSD and *St*DSD-T166A) and closed (SeMet-*St*DSD) forms is highlighted. In the apo-*St*DSD and SeMet-*St*DSD, a sulfate molecule (yellow ball and stick) occupies a position corresponding to 5′ phosphate (orange ball and stick) of PLP in holo-*St*DSD-T166A. (For interpretation of the references to colour in this figure legend, the reader is referred to the Web version of this article.)

including Glu303 (3.08 Å), Cys309 (3.13 Å), Cys276 (3.16 Å), Gly277 (2.87 Å), Leu338 (3.13 Å) and Val340 (3.47 Å) (Supplementary Fig. S2). The metal ion was refined to a B-factor of 18 $Å^2$ comparable with the B-factor of the nearby residues (14–20 $Å^2$). It was proposed that the metal ion might stabilize the PLP binding loop because of its interaction with a residue from the loop *ie* Gly277 and nearby Cys276 [12]. However, in the WtDSD structure, residues surrounding the metal binding site as well as the PLP binding loop were ordered even in the absence of the metal ion suggesting the metal ion may not be required for stabilization of these segments.

3.4. Inter-domain movements

*St*DSD-T166A represents the first holo form of the enzyme. The

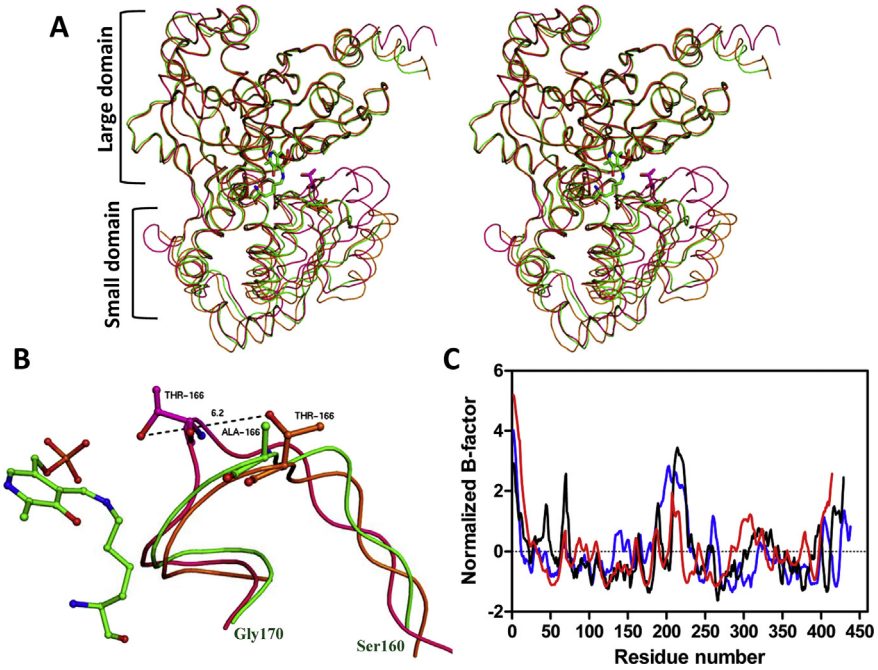

Fig. 3. A. Stereodiagram representing superposition of the Wt-*St*DSD (orange), SeMet-*St*DSD after interaction with isoserine (pink) and holo-*St*DSD-T166A (green) structures. Each protomer has a large and a small domain. Conformational changes may be viewed as a movement of the small domain against the larger domain. **B.** Close up view of the residues (160–170) from the small domain that undergo structural transition upon open to close conformational change of the protein. In Wt-*St*DSD (orange ribbon; open form), the catalytic base Thr166 (orange ball and stick) is far away from the active site. The position of Ala166 (green ball and stick) is unaltered in the T166A mutant (green ribbon; open form). In the closed form (pink ribbon, SeMet-*St*DSD) the small domain undergoes conformational transition bringing the catalytic base Thr166 (pink ball and stick) closer to the cofactor (green ball and stick). This movement is crucial for catalysis. **C.** Comparison of B-factors of Wt-*St*DSD (black), SeMet-*St*DSD (blue) and holo-*St*DSD-T166A (red). The highly disordered residues were not included in the final polypeptide chain and hence B-factors are not available for them. (For interpretation of the references to colour in this figure legend, the reader is referred to the Web version of this article.)

Table 3
The PLP binding affinity of wild type as well as mutant *St*DSD.

Enzyme name	$A_{280\ nm}$	$A_{412\ nm}$	A_{280}/A_{412}
WtDSD	0.1299	0.0148	8.7
T166A	0.1409	0.0132	10.67
D236L	0.1283	0.006	21.38

two previously reported structures were in their apo forms (PDB code: 3R0Z, 3R0X). *St*DSD (PDB code: 3R0Z) represents an open form of the enzyme whereas the SeMet-*St*DSD crystallized in presence of isoserine represents the closed form. The conformational transition could be described as a movement of the small domain against the larger domain (Fig. 3A).

Superposition of the Wt-*St*DSD, SeMet-*St*DSD and holo-*St*DSD-T166A revealed that the structures of Wt-*St*DSD and *St*DSD-T166A are very similar and both of them show substantial differences from SeMet-*St*DSD. Two segments corresponding to residues 160–170 and 180–234 undergo movements of about 5 and 10 Å, respectively, during the structural transition from the open form in Wt-*St*DSD and *St*DSD-T166A to the closed form in SeMet-*St*DSD (Fig. 3A). The deviations observed between Wt-*St*DSD structure and the present PLP-bound structure in the equivalent regions (160–170 and 180–234) are small with a maximum deviation of about 3 Å (Fig. 3A). It was observed that the residue Thr166 (a part of 160–170 segment) undergoes substantial movement when the conformation changes from the open to the closed form. In apo-Wt-*St*DSD and holo-*St*DSD-T166A structures, which are in the open conformation, Thr166 is ~ 8–9 Å away from a modelled D-Ser-PLP external aldimine complex. This distance is too large for Thr166 to function as a proton abstracting residue. However, change of conformation to the closed form as observed in SeMet-*St*DSD brings Thr166 to a distance of 2.6 Å from the Cα position of the ligand, which is favorable for proton abstraction. The relative position of Thr166 with respect to the active site or the internal aldimine in the three different crystal structures is shown in Fig. 3B. The residues 212–227 are disordered in the T166A-*St*DSD and the equivalent residues are ordered in the Wt-*St*DSD. However, they are associated with higher B-factors (above 50 $Å^2$ as compared to 20 $Å^2$ of nearby residues) in Wt-*St*DSD. These features make the active site accessible to PLP and the substrate in the open conformation. The equivalent residues are ordered in the SeMet-*St*DSD with B-factors (~30 $Å^2$) comparable to those of the surrounding residues. Thus, the active site is effectively shielded from the solvent in SeMet-*St*DSD. Normalized B-factors plot (Fig. 3C) and Cα deviation plot (Supplementary Fig. S3A & B) suggest that the main conformational changes are confined to the small domain. It appears that the small domain undergoes a gradual movement from a more open to a less open (upto 3 Å) conformation during apo to holo transition while it undergoes a much larger transition to the closed conformation (upto 10 Å) upon interaction with the substrate/inhibitor. The closed conformation has the appropriate geometry to carry out catalysis.

3.5. The role of Thr166 and Asp236 in catalysis

The wild type *St*DSD and the mutants (T166A, D236L) were expressed in *E. coli* and purified as described in materials and methods. The purified proteins were yellow in colour indicating the presence of PLP in the form of an internal aldimine (absorbance maximum 412 nm). The estimated PLP binding affinities of these mutant enzymes are shown in Table 3. The absorbance peak at 412 nm was lower for D236L mutant as compared to Wt-*St*DSD and T166A-*St*DSD indicating that the D236L mutant has a lower affinity for PLP. The absorbance ratio A_{280}/A_{412} also indicates lower PLP binding affinity of the D236L mutant (Table 3).

This suggests that the residue Asp236 plays an important role in the formation of internal aldimine between Lys116 and PLP. Asp236 is at about 5 Å away from the 5′ phosphate of the internal aldimine suggesting that it might play an important role in stabilizing the

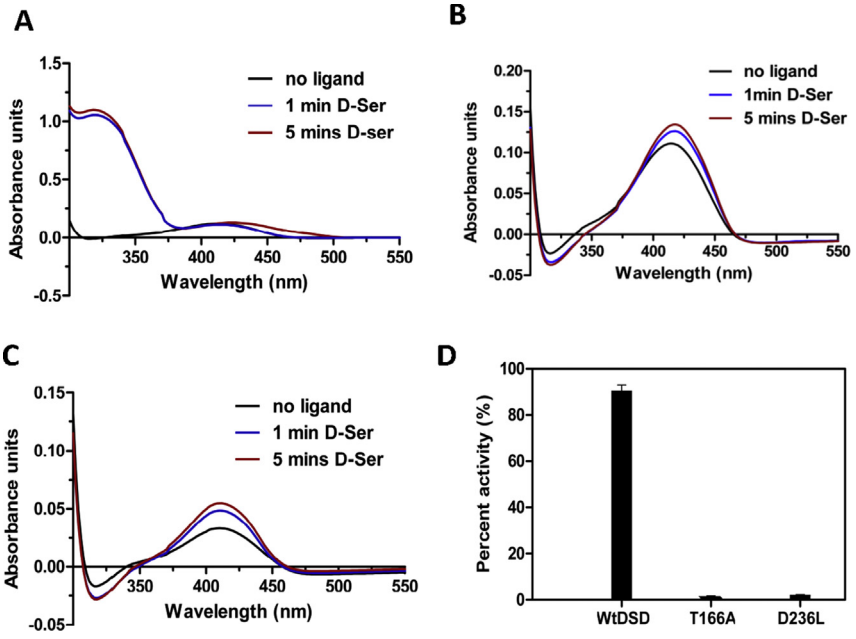

Fig. 4. Spectral studies of Wt-*St*DSD, T166A-*St*DSD and D236L-*St*DSD upon addition of the substrate D-Ser. The absorbance peak at 412–415 nm indicates that the enzyme is bound to PLP (internal aldimine). Appearance of an absorbance peak at 330 nm upon addition of the substrate D-Ser indicates the formation of the product pyruvate suggesting that the enzyme is active. **(A), (B)** and **(C)** indicate the spectral profiles of Wt-*St*DSD, T166A and D236L, respectively, with respect to the substrate D-Ser. Black line corresponds to the spectrum recorded in the absence of the substrate whereas the spectra recorded at 1 and 5 min after the addition of D-Ser are shown in blue and red, respectively. **(D)** Result of DNPH assays carried out to measure the activity of Wt-*St*DSD and the two (T166A and D236L) active site mutants. Both T166A and D236L appear to be inactive enzymes as suggested by both spectral studies and activity assays. (For interpretation of the references to colour in this figure legend, the reader is referred to the Web version of this article.)

internal aldimine.

Spectral studies and activity measurements using 2, 4-DNPH assay were carried out to monitor the activity of the wild type and the mutant enzymes (T166A, D236L) as described in materials and methods. Addition of 1 mM of D-Ser to the Wt-*St*DSD enzyme results in the appearance of an absorbance peak at 330 nm due to the formation of the product pyruvate (Fig. 4A). However, absence of appearance of the corresponding peak upon addition of the substrate D-Ser to T166A-*St*DSD (Fig. 4B) and D236L-*St*DSD (Fig. 4C) indicated that the mutants were inactive. Measurement of percentage specific activity with respect to the Wt-*St*DSD again suggests that both the mutants (T166A, D236L) are inactive (Fig. 4D). Combining the available structural information and biochemical data it is reasonable to suggest the substrate diffuses into the active site in the open conformation of the enzyme. After the formation of the external aldimine complex, the enzyme assumes the closed conformation in which Thr166 is close to the substrate Cα atom. Thr166, which is probably activated by the Lys116, abstracts Cα proton from the external aldimine complex leading to the formation of an aminoacrylate intermediate. In the homologous enzyme serine racemase, Ser82 (structurally equivalent to Thr166 in *St*DSD) has been proposed as the base abstracting proton from D-Ser [22]. Further non-enzymatic cleavage of the aminoacrylate intermediate may lead to the formation of pyruvate and ammonia.

In conclusion, the crystal structure of an active site mutant of *St*DSD (T166A) represents the first holo form of the enzyme from *Salmonella typhimurium*. The holo form resembles the apo or open conformation of the enzyme while the closed conformation is observed upon interaction of the enzyme with isoserine. The active site is accessible to the substrate in the open conformation while it is shielded from the solvent in the closed conformation. The movement of the small domain with respect to the large domain and open to close conformational change is important to bring the base Thr166 close to Cα atom of the substrate. The results presented in this manuscript suggest that Asp236 plays an important role in PLP binding while Thr166 is important for the proton abstraction step of catalysis in DSD.

Acknowledgments

The authors thank Department of Science and Technology (DST, SR/S2/JCB-12/2005/9.5.2006) and Department of Biotechnology (DBT, BT/PR7021/BRB/10/1142/2012), Government of India for financial support. MRN and HSS gratefully acknowledge J.C. Bose and INSA fellowships. GD and SRB were supported by fellowships provided by IISc and CSIR, respectively. The authors also thank the BM14 beamline scientists at ESRF, Grenoble, for collecting the dataset used for the present study.

Appendix A. Supplementary data

Supplementary data related to this article can be found at https://doi.org/10.1016/j.bbrc.2018.08.116.

Transparency document

Transparency document related to this article can be found online at https://doi.org/10.1016/j.bbrc.2018.08.116.

References

[1] J.V. Höltje, Growth of the stress-bearing and shape-maintaining murein sacculus of *Escherichia coli*, Microbiol. Mol. Biol. Rev. 62 (1) (1998) 181–203.
[2] M. Korte-Berwanger, Sakinc Tr, K. Kline, H.V. Nielsen, S. Hultgren, SrG. Gatermann, Significance of the D-serine-deaminase and D-serine metabolism of Staphylococcus saprophyticus for virulence, Infect. Immun. 81 (12) (2013) 4525–4533.
[3] P.L. Roesch, P. Redford, S. Batchelet, R.L. Moritz, S. Pellett, B.J. Haugen, F.R. Blattner, R.A. Welch, Uropathogenic *Escherichia coli* use d-serine deaminase to modulate infection of the murine urinary tract, Mol. Microbiol. 49 (1) (2003) 55–67.
[4] H. Wolosker, E. Dumin, L. Balan, V.N. Foltyn, D-amino acids in the brain: D-serine in neurotransmission and neurodegeneration, FEBS J. 275 (14) (2008) 3514–3526.
[5] M.D. Toney, Controlling reaction specificity in pyridoxal phosphate enzymes, Biochim. Biophys. Acta 1814 (2011) 1407–1418.
[6] D. Dupourque, W.A. Newton, E.E. Snell, Purification and properties of D-serine dehydrase from *Escherichia coli*, J. Biol. Chem. 241 (5) (1966) 1233–1238.
[7] P.L. Roesch, P. Redford, S. Batchelet, R.L. Moritz, S. Pellett, B.J. Haugen, F.R. Blattner, R.A. Welch, Uropathogenic *Escherichia coli* use d-serine deaminase to modulate infection of the murine urinary tract, Mol. Microbiol. 49 (1) (2003) 55–67.
[8] S. Kikuchi, M.A. Ishimoto, D-serine dehydratase acting also on L-serine from *Klebsiella pneumoniae*, J. Biochem. 84 (5) (1978) 1133–1138.
[9] M. Baldassarre, A. Scirè, I. Fiume, F. Tanfani, Insights into the structural properties of D-serine dehydratase from *Saccharomyces cerevisiae*: an FT-IR spectroscopic and in silico approach, Biochimie 93 (3) (2011) 542–548.
[10] H. Tanaka, A. Yamamoto, T. Ishida, K. Horiike, D-Serine dehydratase from chicken kidney: a vertebral homologue of the cryptic enzyme from *Burkholderia cepacia*, J. Biochem. 143 (1) (2008) 49–57.
[11] D.V. Urusova, M.N. Isupov, S. Antonyuk, G.S. Kachalova, G. Obmolova, A.A. Vagin, A.A. Lebedev, G.P. Burenkov, Z. Dauter, H.D. Bartunik, Crystal structure of D-serine dehydratase from *Escherichia coli*, Biochim. Biophys. Acta 1824 (3) (2012) 422–432.
[12] S.R. Bharath, S. Bisht, H.S. Savithri, M.R.N. Murthy, Crystal structures of open and closed forms of D-serine deaminase from *Salmonella typhimurium* implications on substrate specificity and catalysis, FEBS J. 278 (16) (2011) 2879–2891.
[13] G. Deka, S. Bisht, H.S. Savithri, M.R.N. Murthy, Comparative structural and enzymatic studies on Salmonella typhimurium diaminopropionate ammonia lyase reveal its unique features, J. Struct. Biol. 202 (2) (2018) 118–128.
[14] P. Burkhard, G.S.J. Rao, E. Hohenester, K.D. Schnackerz, P.F. Cook, J.N. Jansonius, Three-dimensional structure of O-acetylserine sulfhydrylase from *Salmonella typhimurium*, J. Mol. Biol. 283 (1) (1998) 121–133.
[15] A.R. Shenoy, S.S. Visweswariah, Site-directed mutagenesis using a single mutagenic oligonucleotide and DpnI digestion of template DNA, Anal. Biochem. 319 (2) (2003) 335–336.
[16] The CCP4 suite: programs for protein crystallography, Acta Crystallogr D Biol Crystallogr 50 (Pt 5) (1994) 760–763.
[17] A.J. McCoy, R.W. Grosse-Kunstleve, P.D. Adams, M.D. Winn, L.C. Storoni, R.J. Read, Phaser crystallographic software, J. Appl. Crystallogr. 40 (Pt 4) (2007) 658–674.
[18] G.N. Murshudov, A.A. Vagin, E.J. Dodson, Refinement of macromolecular structures by the maximum likelihood method, Acta Crystallogr D Biol Crystallogr 53 (Pt 3) (1997) 240–255.
[19] P. Emsley, K. Cowtan, Coot: model-building tools for molecular graphics, Acta Crystallogr D Biol Crystallogr 60 (Pt 12 Pt 1) (2004) 2126–2132.
[20] G. Deka, J.N. Kalyani, J.F. Benazir, H.S. Savithri, M.R.N. Murthy, Successful data recovery from oscillation photographs containing strong polycrystalline diffraction rings from an unknown small-molecule contaminant: preliminary structure solution of Salmonella typhimurium pyridoxal kinase (PdxK), Acta Crystallogr F Struct Biol Commun 70 (Pt 4) (2014) 526–529.
[21] A.I. Denesyuk, K.A. Denessiouk, T. Korpela, M.S. Johnson, Functional attributes of the phosphate group binding cup of pyridoxal phosphate-dependent enzymes1, J. Mol. Biol. 316 (1) (2002) 155–172.
[22] M. Goto, T. Yamauchi, N. Kamiya, I. Miyahara, T. Yoshimura, H. Mihara, T. Kurihara, K. Hirotsu, N. Esaki, Crystal structure of a homolog of mammalian serine racemase from *Schizosaccharomyces pombe*, J. Biol. Chem. 284 (38) (2009) 25944–25952.